



## The Fate of Gd (III) Sorption by Novel Microporous Chelating Resin

Ola A. Badr<sup>1\*</sup>, Sameh H. Othman<sup>2</sup>, Mamdouh M. Abo-Mesalam<sup>1</sup>, Azza A. EzzEldin<sup>2</sup>, Tahani I. Kashar<sup>3</sup>,  
Ahmed M. Soliman<sup>1</sup>

<sup>1</sup>. Nuclear Fuel Technology department, Hot Laboratories Centre, Egyptian Atomic Energy Authority.

<sup>2</sup>. Radiation Protection and Civil Defence department, Nuclear Research Centre, Egyptian Atomic Energy Authority.

<sup>3</sup>. Chemistry department, Faculty of Science, Menoufia University



### Abstract

Sorption of Gadolinium (III) by a novel microporous chelating resin Hp-8 from aqueous solutions is investigated in this study at different operating conditions. Characterization of Hp-8 was investigated. Solution pH had a dramatic influence on the uptake in batch process. It was found that pH 2.5 was the best one at the present experimental set. The equilibrium sorption data were fitted to different isotherm models and it is found that both Freundlich and D-R models were able to accurately represent the findings. Based on the D-R isotherm data, the employed resin exhibited maximum adsorption capacity of about 51 mg/g. The three thermodynamic parameters for the present process of adsorption were estimated with values of enthalpy  $\Delta H^\circ = -4.473$ , an entropy  $\Delta S^\circ = -44.127$  and Gibbs free energy  $\Delta G^\circ = -8.597, -9.359, -10.063$  at 298, 318, 328<sup>o</sup>K respectively. Regeneration studies showed that the present resin is effectively applied for sorption of Gd(III) up to 5 cycles.

**Keywords:** Gadolinium separation; Microporous chelating resin; Adsorption; desorption

### 1. Introduction

Numerous recent technologies as consumer communications, electronics, computers and networks, sustainable energy, modern transportation, healthcare, environmental mitigation and national security depend on Earth's crust contains rare earth elements. Of these elements, gadolinium (Gd(III)) is considered as an essential one [1]. Due to its unique characteristics, gadolinium is particularly well suited

for essential tasks like neutron radiography and reactor shielding [2]. As a contrast agent, it is applied to tumours during neutron therapy and magnetic resonance angiography operations. It can also improve magnetic resonance imaging (MRI), aiding in the treatment and detection of cancer [3]. Gadolinium is a rare earth element that is frequently used in X-rays and bone density testing,

\*Corresponding author e-mail: [olabadr91@gmail.com](mailto:olabadr91@gmail.com). (Ola A. Badr)

Received date 06 December 2022; revised date 14 December 2022; accepted date 14 December 2022

DOI: [10.21608/EJCHEM.2022.174488.7191](https://doi.org/10.21608/EJCHEM.2022.174488.7191)

©2023 National Information and Documentation Center (NIDOC)

contributing significantly to modern medical advancements [4]. It's also helpful in nuclear technology for fabricating fuel elements, control rods, refractory materials, ceramic industries, metallurgy and serves as neutron poison in reactors using heavy water. When injected into the heavy water moderator at a quantity of 15 g/ml during an emergency shutdown and 2 g/ml when the reactor is first started [5]. Gadolinium (III) separation and purification are essential for all of the above mentioned uses.

Utilizing organic chemical resin is one of the useful methods for element separation along with a number of other methods such as volatilization, liquid-liquid extraction, precipitation/coprecipitation, column chromatography, cloud point extraction, solvent extraction, nanofiltration and electrolysis [6-18]. Ion exchange resins are broadly categorized as chelating resins. Chelating groups and polymer matrix make up the majority of it. Organic polymers found in polymer matrix are insoluble but frequently swell in water and a variety of organic solvents.

The most common cross-linked synthetic organic polymers utilized as matrices are styrene-divinylbenzene copolymers. For the adsorption of elements from solutions, chelating resin is offered for batch and flow techniques [19].

This study aims to evaluate the performance of a commercial microporous chelating resin for use as a sorbent to Gd(III) using aqueous solutions with maximum adsorption capacity equal to 51 mg/g. (Madbouly HA et al, 2018) could separate terbium(III) and gadolinium(III) from aqueous nitrate medium using (TVEX-PHOR) with resin uptake capacity (15.49 mg/g) for Gadolinium [20]. Also adsorption of Gadolinium from H<sub>2</sub>O and HCl solutions on ion-exchange resin C100 was studied with maximum adsorption capacity amounted to 1.2 ± 0.1 mmol g<sup>-1</sup> [21].

The result of multiple variables (solution pH, initial concentration and contact time) on sorption efficiency is explored. Desorption studies for Gd(III)-loaded resin and the thermodynamic parameters of sorption process were calculated.

## 2. Experimental

### 2.1. Materials

The reagents used in this investigation were of analytical reagent high purity, which meant they didn't need to be purified any further. The working solutions were prepared using distilled water. The resin employed in this study is a kind of crosslinking functional polymer material which can form multi-coordination complex with metal ions. It's a heavy metal chelating resin that removes heavy metals from water and appears as a white globular particle with water content of 50.0-60.0%, granularity range 0.4-1.20(mm) ≥ 95.0%, wet visual density 0.75-0.85g/mol, sphericity ≥ 95.0%, skeleton density 0.8-1.0g/mol.

5200 mg/l gadolinium (III) ions stock solution was made by dissolving the proper amount of gadolinium oxide. After that, it was diluted to the preferred concentrations then pH was adjusted as needed with solutions of hydrochloric acid or sodium hydroxide. A Shimadzu UV-visible spectrophotometer was used to measure the amounts of the examined components in the aqueous phase (model uv-160 1PC, Gemen). Gd(III) ions were standardized and spectrophotometrically determined at 650 nm employing Arsenazo (III) technique at 25 °C and pH 3.5 buffer solutions. The pH was adjusted for a buffer in presence of 1% ascorbic acid [22].

## 2.2. Adsorption studies

The quantitative uptake of gadolinium by the chelating resin was investigated using batch sorption experiments. As analytical variables, pH, time, temperature, sorbent/solution volume ratio (S/L), and Gd(III) initial concentration have all been studied. The removal percentage (Removal%) of Gd(III) was determined by comparing the Gd(III) concentration in the aqueous solution before and after the sorption process at the equilibrium time  $t$  according to the following relation[23]:

$$\text{Removal \%} = \frac{C_0 - C_e}{C_0} \times 100 \quad (1)$$

$C_0$  and  $C_e$  for the initial and equilibrium concentrations of Gd(III) in the solution, in milligrams per litre, respectively. Based on difference between equilibrium and Gd(III) initial concentration along with ( $V$ ) volume of the solution and ( $m$ ) mass of resin which have the units L and g, respectively, Gd(III) amount sorbed  $q_e$  (mg/g) was determined as:

$$q_e = (C_0 - C_e) \times \frac{V}{m} \quad (2)$$

On the other hand,  $K_d$  distribution coefficient (ml/g) was estimated using this equation [24]:

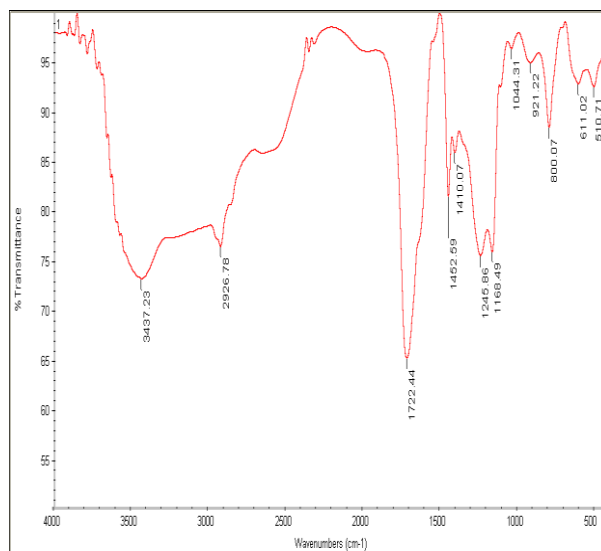
$$K_d = \frac{(C_0 - C_e)}{C_e} \times \frac{V}{m} \quad (3)$$

## 3. Results and discussion

### 3.1. Characterization of Hp-8 resin

According to the examination of the principal absorption spectra for Hp-8 resin shown in Fig. 1, the resin has the following structure and composition: N-H stretching of secondary amine that is indicated by the big absorption peak at  $3437.23 \text{ cm}^{-1}$ . The peak at  $2926.78 \text{ cm}^{-1}$  shows C-H stretching of alkane ( $-\text{CH}_3$ ). The peak at  $1722.44 \text{ cm}^{-1}$  is a strong peak shows C=O stretching and the absorption bands

from  $1044.31$ ,  $1168.49$  and  $1245.86 \text{ cm}^{-1}$  are clearly attributed to the stretching and asymmetric vibrations of the  $\text{SO}_3$ -sulphonic group.



**Figure(1):FTIR spectra of Hp-8 resin before adsorption of Gd(III)**

The TGA–DTA data diagram of the resin in figure (2) were performed using nitrogen (flow rate, 20 mol/min) at a heating rate of  $20^\circ \text{C}/\text{min}$ .

According to the TGA curves in the current work, there are three temperature ranges observed in which the majority of the weight variations for Hp-8 resin occur. At first there is weight loss about 5.87% at temperature  $112.87$  to  $242.12^\circ \text{C}$ , then fast degradation with weight loss about 23.574% at temperature around  $344.89^\circ \text{C}$  leaving remaining mass about 70.513% and finally complete degradation with weight loss 42.004% at temperature higher than  $502.73^\circ \text{C}$

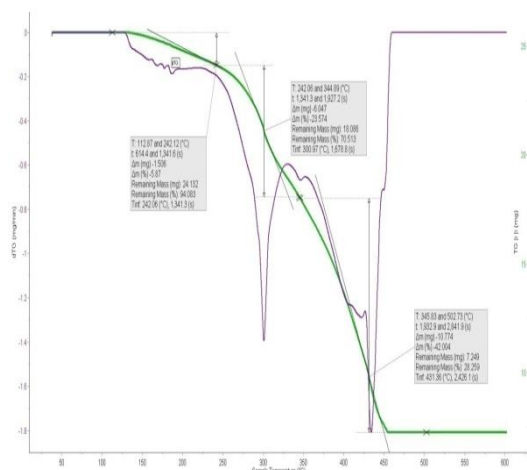


Figure (2): TGA-DTA for Hp-8 resin.

### 3.2. PH Effect

Solution's initial pH has a significant impact on metal adsorption because it controls resin's surface binding site and aqueous charge distribution. For 50 mg/L Gd (III) initial concentration, pH effect on the adsorption behaviour of the chelating resin was tested by altering initial pH from 1 to 5 at 25°C. Data that obtained are depicted in Fig. 3.

The figure represents that the percent of the removal of Gd(III) is increased with pH, and removals are almost completely achieved at a pH of 2.5. The reduction in the sorption efficiency at the lower studied pH values can be attributed to that H<sup>+</sup> and Gd<sup>3+</sup> ions compete with one another to bind to the functional groups of the resin.

Fig. 1 also shows that the final pH after adding the resin to the metal ions solution is not affected much and this is due to the fact of acidity of resin groups. As a result, batch studies of the subsequent experiments were carried out at an initial pH of 2.5.

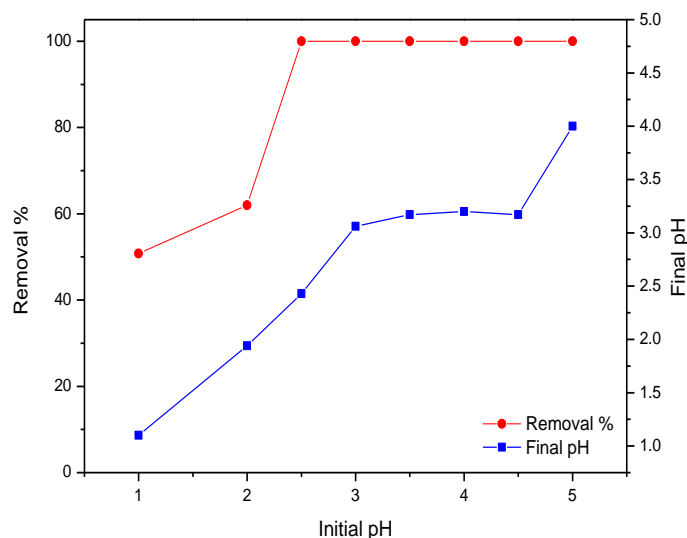


Figure (3): pH effect on the percent removal of 50 mg/l Gd(III) on the resin at room temperature and one day of contact.

### 3.3. Adsorbent dosage effect

Figure (4), illustrates how the resin dose affects how many Gd ions are taken up by the resin and how much of them are removed from the solution.

The degree of metal adsorption was considerably influenced by the resin dose used, as seen in the figure, where the values of  $q_e$  rose with increasing adsorbent mass. For a change in resin dose from 0.01 - 0.1g, the removal percentage (% Gd) rose from 69.4% to 100%.

The percentage of gadolinium ions removed from the aqueous media increased as the dosage of microporous resin was increased because more sorption sites became accessible for sorbent-solute interaction.

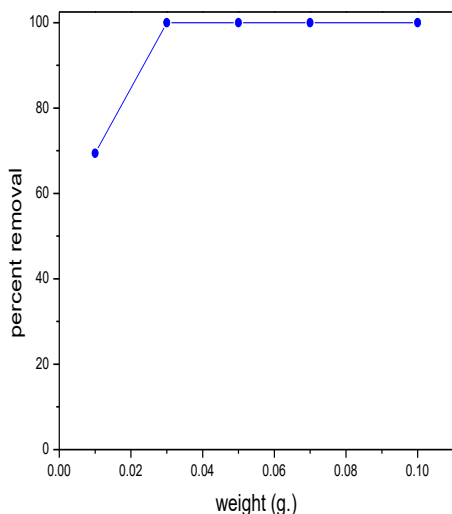


**Figure (4): Adsorbent dosage effect on Gd(III) sorption with the chelating resin at pH of 2.5 and 25°C.**

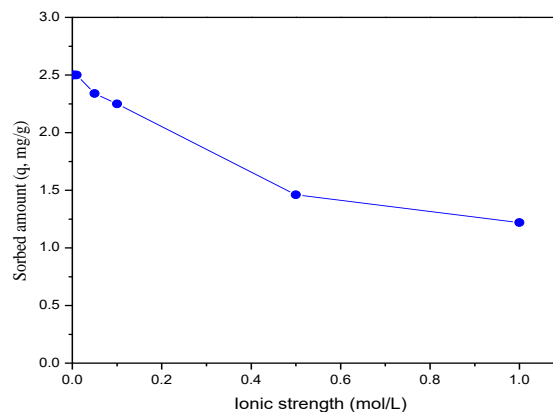


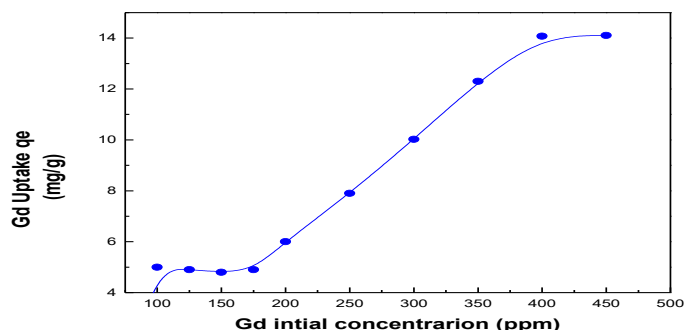
**Figure (5): Variation of the sorbed amount of Gd(III) with ionic strength of the solution.**

### 3.4. Effect of ionic strength

$\text{Na}^+$  ions are the dominant ions that present as foreign ions in most of liquid waste of heavy metal industries, so several experiments were carried out where this ion at concentrations ranging from  $5 \times 10^{-4}$  to 1 mol/L. The remaining variables in these studies were kept consistent, such as utilizing 5 mL of 50 mg/L gadolinium with 0.1 g resin at room-temperature and one day contact time. The obtained findings show that the sorption of gadolinium decreases with  $\text{Na}^+$  ions concentration increase. The ability of Gd(III) and  $\text{Na}^+$  to compete on the resin may be attributed to the fact that  $\text{Na}^+$  has the smallest radius, the highest affinity for the resin's surface, and has the greatest susceptibility for chelation with the surface groups of the resin. All that mentioned reduce the quantity of ion interaction sites with Gd on resin surfaces [25]

### 3.5. Initial concentration effect of Gd(III) on adsorption process

It was also discovered that metal ion initial concentration improved the capacity of resin to remove metal at equilibrium. Gd(III) distribution coefficients was found to substantially rise with the change in metal ion concentration over the range of 50 to 500 mg/l, and as a result, the adsorption capacity increased until it reached its



maximum capacity (fig.6)

**Figure (6): Effect of various concentrations of Gd(III) with pH 2.5, contact time of one day**

### 3.6. Time effect on adsorption process

On the polymeric resin, sorption tests were performed using an adsorbent dose of 0.1g. The initial adsorption of Gd(III) by resin was quite quick. The vast quantity of vacant sites available during the exchange's early phase may have contributed to the initial quick phase. The quantity of Gd(III) adsorbed, however, rises over time and stabilizes after about 22 hours. The quantity of Gd(III) adsorbed did not significantly alter over time beyond the equilibrium time. Thus, 22 hours were chosen for all further research (fig.7).

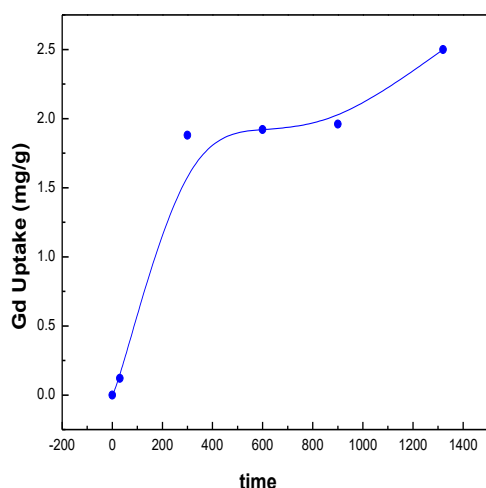


**Figure (7): Contact time effect with Gd concentration 50mg/l and pH :2.5.**

#### 3.6.1. Adsorption kinetics study

Data from the equilibrium were treated according to four famous kinetic models in order to determine the kinetics of Gd(III) adsorbed on the resin over time. Frequently, the results of experiments using pseudo-first-order Eq. (4), pseudo-second-order Eq.(5), the intra-particle diffusion Eq. (6), and the Elovich model

Eq.(7) are modelled to demonstrate the rate-limiting step is either adsorption or diffusion[26]. The following equation represents the kinetic model of Pseudo-first-order :

$$\log(q_e - q_t) = \log q_e - \frac{k_1}{2.303} t \quad (4)$$

Pseudo-first-order adsorption rate constant is  $K_1$  in ( $\text{min}^{-1}$ ), the quantity of ions of metal adsorbed at equilibrium is  $q_e$ , and the amount of ions adsorbed at time (t) is  $q_t$ . A linear relationship of  $\text{Log}(q_e - q_t)$  versus (t) that can be used to calculate  $K_1$  and  $q_e$  value from the slope and intercept respectively, and has indicated that the actual results can be fit using the kinetic model of pseudo first order.

The estimated adsorption capacity value ( $q_e$ ) was found to be more than the practically established capacity. As a result of these findings, the kinetic model of first order is inappropriate for the system under consideration since it does not match the experimental findings.

Even though the plot's straight lines indicate that the model can explain the results of the experiment with high correlation coefficients, the theoretical sorption capacities, or  $q_e$  the calculated values for the Gd(III) ions under consideration do not match  $q_e$  (experimental) values. Therefore, this may suggest that the sorption of Gd(III) onto the resin does not follow this model.

Compared with the equation of pseudo second order that's described by:

$$\frac{t}{q_t} = \frac{1}{k_2 \times q_e^2} + \frac{1}{q_e} t \quad (5)$$

The pseudo second order adsorption rate constant is  $K_2$  in ( $\text{g}/\text{mg} \cdot \text{min}$ ) and the rate parameter is thus determined by testing the plot's straight line of  $t/q_t$  versus t. It is evident that the experimental results and

the computed values are in good accord. The kinetic model of pseudo second order provides a better explanation of the kinetics of Gd (III) ions adsorption based on data analysis. As a result, it's possible that gadolinium ions adsorption fits the pseudosecond order kinetic model. Thus, the values of  $q_e$  (experimental) are more similar to  $q_e$  (calculated). In addition, table (1) demonstrate that  $R^2$  (correlation coefficient) for Gd(III) ions has a high value very close to unity and indicate the data of the above mentioned models' mathematical parameters.

**Table (1): pseudo-first-order and pseudo-second-order kinetic parameters for Gd(III) sorption on the resin.**

Pseudo first order reaction				Pseudo second order reaction			
$q_e$ Exp (mg/g)	$q_e$ Cal. (mg/g)	K (g/mg min)	$R^2$	$q_e$ Exp (mg/g)	$q_e$ Cal. (mg/g)	$K_2$ (g/mg min)	$R^2$
2.5	1.8	0.0032	0.980	2.5	2.03	0.034	0.999

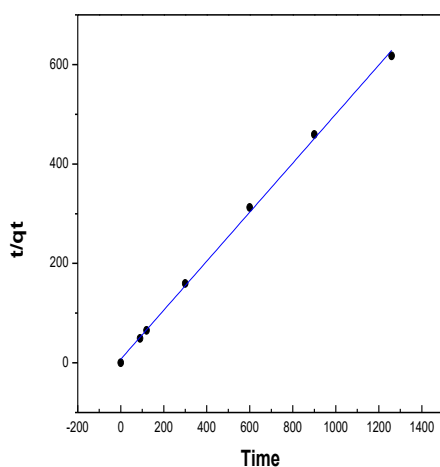


**Figure (8): Kinetics of pseudo-first order for Gd (III) sorption on the resin: amount of resin 0.1g, conc. 50 ppm, pH 2.5.**

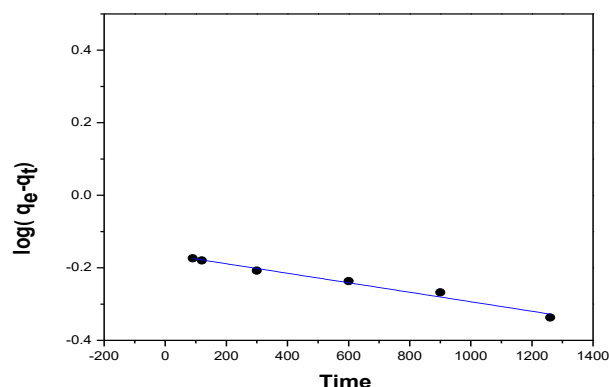


**Figure (9): Kinetics of Pseudo-second order for Gd (III) sorption on the resin. Amount of resin 0.1 g, conc. 50 ppm and pH 2.5.**

To demonstrate the impact of intra-particle diffusion on the rate of adsorption (Weber and Morris 1963) by the third kinetic equation [27]:

$$q = k_1 t^{0.5} + C \quad (6)$$

For the Weber-Morris intra particle diffusion kinetic model, the plot of  $q_t$  against  $t^{1/2}$  results in straight lines, as seen in figure (10). For Gd(III) ions, the value of  $K_{ad}$  is determined by the straight line's slope that is  $0.07 \text{ mg/g min}^{1/2}$  and  $C$  (the intercept) is  $0.15 \text{ mg/g}$ , as in table (2).

Since  $R^2$  is far from the unity, the kinetic model of intra-particle diffusion cannot be applied to Gd(III) ions and is not the rate-controlling step for metal ions. The boundary layer thickness decreases as  $C$  decreases.

Additionally, the difference in the mass transfer rate between the initial and final phases of adsorption may contribute to the straight line deviation of from the origin. The graphs were not straight across the entire time period, showing that the adsorption was impacted by many processes.

Elovich kinetic model is represented by:

$$q_t = \frac{1}{b} \ln ab + \frac{1}{b} \ln t \quad (7)$$

The initial adsorption rate constant is (a) in (mg/g.min) and the constant related to the extent of metal ions surface coverage and adsorption process activation energy for is b [28].

In figure (11), the plot of  $q_t$  against  $\ln t$  results in a straight relationship. Values of (a and b) for Gd ions can be obtained from the slope and intercept respectively. The previous tables (1,2) demonstrate that the kinetic model of pseudo-second order have greater correlation coefficient  $R^2$  value than the first models. The equilibrium adsorption capacity predicted is also extremely similar to the experimental value, suggesting that the kinetic model of pseudo-second order is a better fit for the sorption kinetics onto the resin. This implies that the phase of rate-limiting in the metal ions adsorption process contributes valence interactions by donating or exchanging electrons in between Gd(III) ions and the resin.

**Table (2): Weber–Morris intra-particle diffusion and Elovich models Kinetic parameters for Gd(III) ions sorption.**

The intraparticle diffusion model			Elovich model		
$k_{ad}$ (mg/g min <sup>1/2</sup> )	C (mg/g)	$R^2$	a (mg g <sup>-1</sup> min <sup>-1</sup> )	b (g mg <sup>-1</sup> )	$R^2$
<b>0.07</b>	<b>0.15</b>	<b>0.947</b>	<b>9.8</b>	<b>1.8</b>	<b>0.903</b>

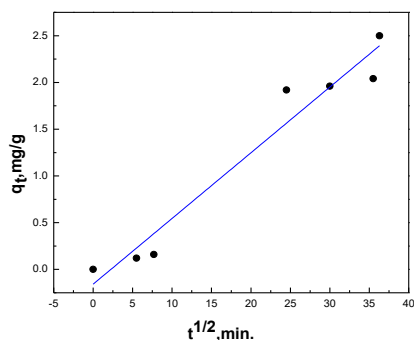


**Figure (10): Intra-particle diffusion model for Gd(III) adsorption onto the resin.**

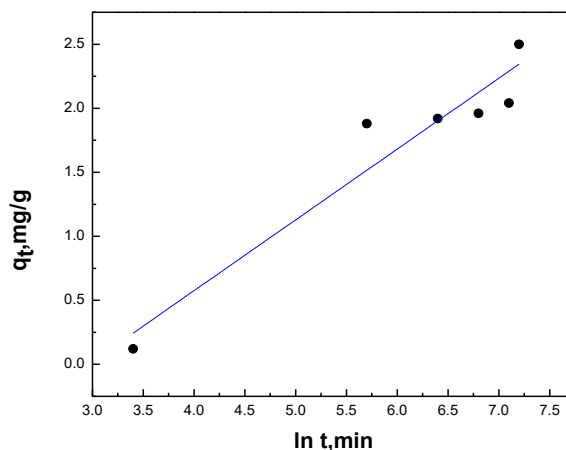


**Figure (11): Gd(III) adsorption Elovich kinetic model.**

### 3.6.2. Adsorption isotherm study

A specific relationship between the adsorbed Gd metal ions and its aqueous phase equilibrium concentration was used to measure the resin adsorption capacity under the given experimental conditions of resin 0.1 g versus 50 mg/l Gd concentrations for one day contact time at room temperature and with pH adjusted at 2.5. The two isotherms of Freundlich and Langmuir are that are most frequently utilized. On the adsorbent surface, a saturated monolayer of adsorbate molecules, where constant energy of adsorption and zero adsorbate transmigration occurs on the surface's plane, is what the model of Langmuir defines as maximum adsorption. The following formula gives a description of it [29].

$$\frac{c_e}{q_e} = \frac{1}{k_1 Q^0} + \frac{1}{Q^0} \times c_e \quad (8)$$

The solution equilibrium concentration in (mg/L) is  $C_e$ , the adsorption capacity monolayer (mg/g) is  $Q^0$ , and the Langmuir constant relating to the metal affinities of the binding sites is  $K_1$ . In figure (12) The graph of  $C_e/q_e$  versus  $C_e$  of the investigated metal ions

is shown. The Langmuir plot's linear regression fits suggested that the Langmuir model is incompatible with the experimental results.

When applied to heterogeneous adsorbent surfaces, the Freundlich isotherm equation implies that the sites of binding are either independent or equal [30].

Freundlich isotherm can be described by a common form:

$$\log q_e = \log K_f + \frac{1}{n} \log c \quad (9)$$

$K_f$  and  $n$  represent the capacity of adsorption (mg/g) and adsorption intensity respectively and the Gadolinium amount adsorbed per unit mass of resin is  $q_e$ . A linear plot of  $\log q_e$  against  $\log c_e$  yields  $K_f$  and  $n$  as well.

The results supported the model of Freundlich isotherms since  $R^2$  for Freundlich isotherm is closer to one than that for the model of Langmuir isotherm. Also, the  $1/n$  number typically based on the distribution of active sites, the kind and intensity of the sorption process, and these factors together. The metal ion Freundlich isotherm's slope ( $1/n$ ), as shown in Table 3, is between 1 and 10, it has also shown a preferential adsorption of Gd ions onto the resin, demonstrating that the bond energy rises as surface density does [31]. This demonstrated effective metal ions adsorption on the resin.

The sorption capacity value  $q_e$  (exp.) determined by equations differs significantly from that deduced from the Freundlich isotherm. This gap is caused by the fact that  $K_f$  is the relative adsorption capacity that indicates the selectivity order for gadolinium ions under investigation. The apparent capacity ( $q_e$ ) is a numerical representation of the resin's capacity strength for Gd(III). Because of the straight lines produced by the Freundlich isotherm, it is presumed that the adsorption of active sites and interactions

between sorbed molecules with a heterogeneous energy distribution.

It is possible to distinguish between physical and chemical adsorption using the Dubinin-Radushkevich (DR) isotherm model's linear form to better understand the nature of the adsorption process [32].

$$\ln q_e = \ln q_m - \beta \varepsilon^2 \quad (10)$$

Where  $q_m$  the maximal theoretical monolayer saturation capacity (mg/g). Dubinin-Radushkevich model constant is  $\beta$  in ( $\text{mol}^2 \text{kJ}^{-2}$ ) and the Polanyi potential is  $\varepsilon$  have the following formulas, which are linked for each sorbed molecule's average free adsorption energy:

$$\varepsilon = RT \ln \left( 1 + \frac{1}{C_e} \right) \quad (11)$$

The equilibrium concentration of adsorbate in solution is  $C_e$  in (mol/L), general gas constant is  $R$  ( $8.314 \times 10^{-3} \text{ kJ mol}^{-1} \text{ K}^{-1}$ ), and the absolute temperature  $T$  (K). It is possible to determine the values of  $q_{\text{max}}$  and  $\beta$  by evaluating intercept and slope of the linear plot of  $\ln q_e$  against  $\varepsilon^2$ . The sorption mean free energy,  $E$  in (kJ/mol), which is the change in free energy needed to transport one mole of ions to the solid surface from the solution, is linked to of  $\beta$ . As stated, this relationship is:

$$E = \frac{1}{\sqrt{2\beta}} \quad (12)$$

( $E$ ) can detect the mechanism of the reaction. These are somewhat below the standard indicated that a physisorption mechanism, which is 8.0 kJ/mol.

In addition, this suggests that a physisorption process is responsible for the interaction of the metal ions with the resin's active sites. The impact of temperature will contribute to the ultimate conclusion [33].

**Table (3): The sorption of Gd(III) with the (D-R), Freundlich, and Langmuir parameters on the resin.**

Langmuir model			Freundlich model			D-R model		
b (L/mg)	Q <sub>o</sub> (mg/g)	R <sup>2</sup>	1/n	K <sub>f</sub> (mg/g)	R <sup>2</sup>	q <sub>m</sub> (mg/g)	E (KJ/mole)	R <sup>2</sup>
<b>0.03</b>	<b>14.3</b>	<b>0.5</b>	<b>1.</b>	<b>0.1</b>	<b>0.9</b>	<b>50.9</b>	<b>7.07</b>	<b>0.9</b>
<b>7</b>		<b>73</b>	<b>3</b>		<b>96</b>			<b>89</b>

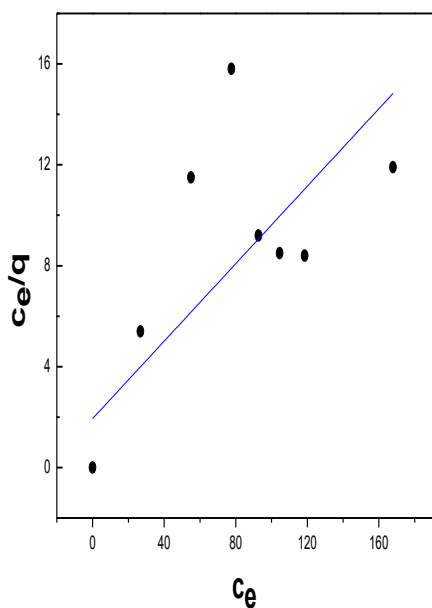


**Figure (12): Plot of Langmuir isotherm for Gd(III) metal ions adsorption on the resin, weight of resin 0.1g ,pH 2.5 at 25<sup>o</sup>c**

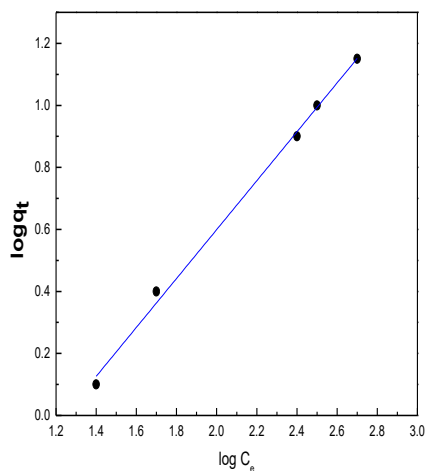
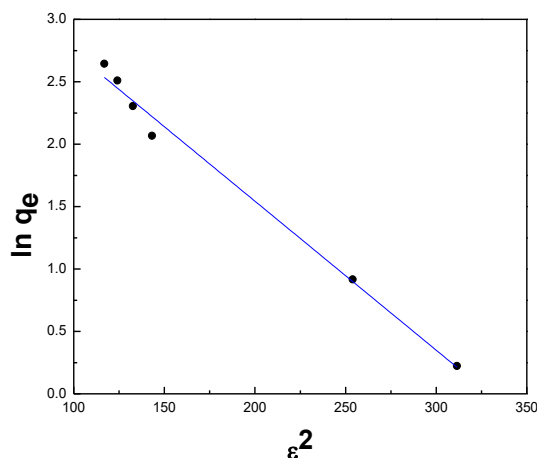


**Figure (13):Plot of Freundlich isotherm for Gd(III)metal ions adsorption ontheresin, weight of resin 0.1g, pH 2.5 at 25<sup>o</sup>c**



**Figure(14): Plot of D–R isotherm for Gd(III) metal ions adsorption on the resin, weight of resin 0.1g, pH 2.5 at 25<sup>o</sup>c**

### 3.6.3 Adsorption thermodynamic study

It was investigated how temperature affected the absorption of Gd(III) by adding 0.1g of the resin with 250 mg/L metal ions at temperatures 298 - 328<sup>o</sup> K at pH 2.5, and 22hourscontact time(the previously specified optimum conditions).

In Fig. (15), as the temperature rises between 25 and 55°C, metal adsorption rises, which was shown as a relationship between  $\ln K_c$  and  $1/T$  the absolute temperature reciprocal, where  $K_c$  is the constant of sorption process's equilibrium.

The Gibbs free energy  $G$  (kJ/mol), the enthalpy  $H$  (kJ/mol), and the entropy  $S$  (J/mol.K) of this system were calculated using the following Vant Hoff equation [34].

$$\ln K_c = \frac{-\Delta H}{RT} + \frac{\Delta S}{R} \quad (13)$$

The distribution coefficient is  $K_d$  in (mL/g), the universal gas constant is  $R$  and equal (8.314 J/mol.K) and  $T$  represent temperature in (K). The equilibrium constants' ( $\ln K_c$ ) plots against  $1/T$  provides a linear relationship with a slope ( $H/R$ ) and intercept ( $S/R$ ) that can be used to determine  $\Delta S^\circ$  (J/mol/K), and  $\Delta H^\circ$  (J/mol), while the Gibbs free energy,  $\Delta G^\circ$  (KJ/mol), is calculated from the following equation:

$$\Delta G = -RT \ln K_c \quad (14)$$

**Table (4): Parameters of the thermodynamic system for Gd (III) adsorption on the resin, amount of resin 0.1 g and pH=2.5.**

T (K)	$\Delta H$ (kJ/mol)	$\Delta S$ (kJ/mol K)	$\Delta G$ (kJ/mol)
298	-4.473	-44.127	-8.597
318			-9.359
328			-10.063

The tabulated results demonstrate that negative change in enthalpy values declared the nature of metal ions sorption is exothermic, but negative entropy change values imply a decrease in the reaction system's disorder and suggest the likelihood of favourable sorption. Furthermore, The process' spontaneity is revealed by the estimated negative

values of the free energy change [35]. For physisorption the standard free energy change  $\Delta G$  ranges from 20 -0 kJ mol<sup>-1</sup>, while for chemisorption; it ranges from 80 - 400 kJ mol<sup>-1</sup>. The total  $\Delta G$  for Gd(III) in the current investigation ranges between - 8.597 and -10.063 kJmol<sup>-1</sup>. These findings demonstrate that this system does not rely on external energy sources and support a physisorption of the gadolinium ions that happened spontaneously [36].

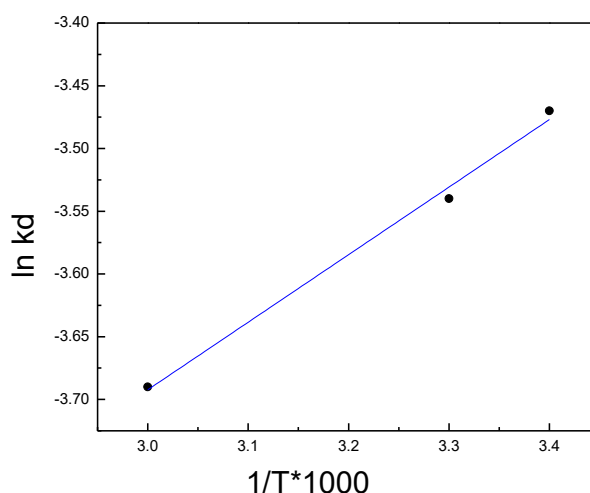


**Figure (15):  $\ln K_{av}$  vs  $1/T$  of Gaddolinium(III) sorption upon the resin**

The exponential factor  $e^{-E_a/RT}$  in the Arrhenius equation determines the percentage of molecules with energy equal to or greater than  $E_a$  [37]:

$$K = Ae^{\frac{-E_a}{RT}} \quad (15)$$

$E_a$  is the activation energy; frequency factor constant or also known as pre-exponential factor or Arrhenius factor is  $A$ . It illustrates the collision rate and the percentage of collisions with the necessary orientation for the reaction to take place.

The rate constant  $k$  has the same unit as  $A$ , and its value fluctuates depending on the response sequence.

According to the plot of Arrhenius for the adsorption, the activation energy is almost equal to 5 kJ/mol, which is within the energy range of 5–40 kJ/mol. According to the result, a counter ion exchange mechanism is the type of adsorption onto the resin. Once more, quick kinetic adsorption is indicated by low activation energy [38].

### 3.7. Desorption studies

The metal ions' desorption efficiency allows the resin to be reused and the metal to be recycled. Studies on desorption and regeneration were also done to investigate the possibility for pre-concentration.

After Gd(III) sorption by the resin, the sorbed metal was subsequently desorbed using 5 ml of mineral acid HCl ranging from 0.01 to 1 M. HCl, NaCl and CaCl<sub>2</sub> solution at 25°C with a contact duration of one day that's adequate to achieve desorption equilibrium. At low pH levels, Gd is typically in the form of an ion with a positive charge; however, at higher pH levels, it starts to precipitate as hydroxide.

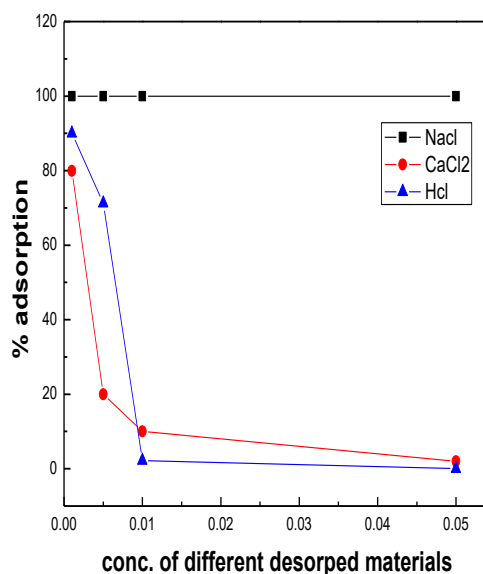
The use of HCl solutions increases the concentration of protons since they have a positive charge at low pH levels. Meanwhile, Gd in positively charged form is more readily extracted by H<sup>+</sup>, resulting in ion transfer desorption of adsorbed Gd.

As a result, 0.01 M HCl was shown to be an effective desorbing reagent for eluting the adsorbed ions from the resin with the greatest desorption efficiency of nearly 100% towards Gd(III). The oxygen atom's lone pair on the resin may be contributed to the vacant Gd(III) atomic orbital in low acidic solution, causing complexes with metal ions to form on the

adsorbent surface. As a result, cationic form of metal ions predominate in the acidic media, and the process of elution is simple.

In other words, when adsorbed Gd was treated with 0.01 M hydrochloric acid, adsorption process occurred due to a competition between the metal ions cationic form and H ions given by HCl solution, resulting in H<sup>+</sup> occupying active sites. It has an effect on the resin's ability to bind metals, and the majority of Gd(III) returns to the solution. As a result, 0.01 M HCl may be regarded as an excellent eluent for Gd(III), and resin reuse is greatly increased.

The metal ions adsorption-desorption cycle was performed more than three times using the same beads to demonstrate the adsorbent's reusability..



**Figure(16):Desorption of Gd(III)-loaded resin using different desorbing agents.**

During repeated adsorption-desorption processes, the resin's adsorption capabilities did not vary substantially. These findings indicate that the resin has a high capacity for regeneration

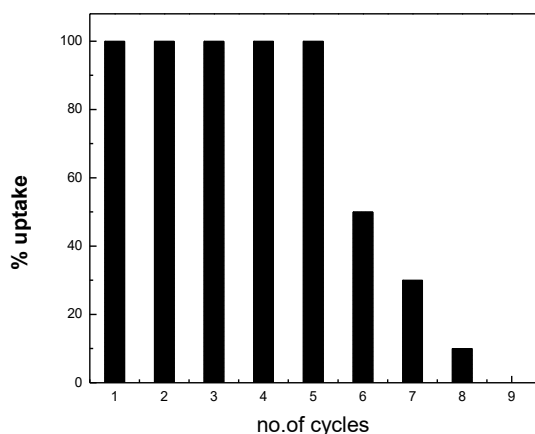


**Figure (17): number of cycles for Gd(III) adsorption with resin weight = 0.1 g, pH 2.5 and temp. of 25°C.**

#### 4. Conclusion

Hp-8 microporous chelating resin can be used as an efficient and economical sorbent to remove Gd(III). Its sorption came to an equilibrium in 22 hours. The kinetic data showed that pseudo-second-order was appropriate for this resin in the sorption of Gd ions. Freundlich model was shown to accurately reflect the sorption equilibrium from the isotherm investigations. From our findings there's a physical adsorption between Gadolinium atoms and the resin's binding sites for several reasons as adsorption occurred at low pH, The sorption mean free energy,  $E$  calculated from D-R  $< 8$  kJ/mol and  $\Delta G$  values for adsorption process 20-0 kJ/mol. The sulphonate group (the major group on the resin) binded physically with Gadolinium atoms.

While the determined entropy change's negative sign showed that the adsorption mechanism through electrostatic contact between the adsorbent surface

and the adsorbate species in the solution. thermodynamic analysis suggested that the sorption process is spontaneous and exothermic. According to studies of desorption, the resin may be developed and employed more than five times for further sorption procedures, and a 0.01 M HCl solution can be used to desorb Gd ions from the resin. The resin's maximum sorption capacity was 2.5 mg per 0.1 g of resin at pH = 2.5.

#### Conflict of interest

Each author certifies that they have no conflict of interest.

#### References

- 1- Bielawski, Radosław. "Rare earth elements—a novelty in energy security." *Journal of Ecological Engineering* 21, no. 4 (2020).
- 2- Burke, D. S., and S. H. Byun. "Feasibility of gadolinium oxide paint as neutron shielding." *Nuclear Instruments and Methods in Physics Research Section A: Accelerators, Spectrometers, Detectors and Associated Equipment* 1025:166175(2022). <https://doi.org/10.1016/j.nima.2021.166175>
- 3- Narmani, Asghar, BagherFarhood, HamedHaghi-Aminjan, TohidMortezazadeh, Akbar Aliasgharzadeh, MehranMohseni, MasoudNajafi, and HadisAbbasi. "Gadolinium nanoparticles as diagnostic and therapeutic agents: Their delivery systems in magnetic resonance imaging and neutron capture therapy." *Journal of Drug Delivery Science and Technology* 44: 457-466(2018). <https://doi.org/10.1016/j.jddst.2018.01.011>
- 4- Huang, Yongkang, XinyunZhai, Tengfei Ma, Mengzhen Zhang, Haobo Pan, William Weijia Lu, Xiaoli Zhao et al. "Rare earth-based materials for bone regeneration: breakthroughs and

- advantages." *Coordination Chemistry Reviews* 450:214236 (2022).<https://doi.org/10.1016/j.ccr.2021.214236>
- 5- Borai, Emad, MikkoKaresoja, and RistoHarjula. "Separation of cobalt from europium with mesoporous hybrid silica-poly (styrene) impregnated chelating resin." *Mineral Processing and Extractive Metallurgy Review* 34, no. 1: 57-72(2013).<https://doi.org/10.1080/08827508.2011.623748>
- 6- Korkisch, Johann. Modern methods for the separation of rarer metal ions.Elsevier, 2013.
- 7- Hidayah, NurNadiatul, and SumaiyaZainalAbidin. "The evolution of mineral processing in extraction of rare earth elements using liquid-liquid extraction: A review." *Minerals Engineering* 121: 146-157(2018).<https://doi.org/10.1016/j.mineng.2018.03.018>
- 8- Liu, Tianchi, and Ji Chen. "Extraction and separation of heavy rare earth elements: A review." *Separation and Purification Technology* 276:119263(2021).<https://doi.org/10.1016/j.seppur.2021.119263>
- 9- Neves, Heyder Pereira, Gabriel Max Dias Ferreira, Guilherme Max Dias Ferreira, Leandro Rodrigues de Lemos, Guilherme Dias Rodrigues, VersianeAlbisLeão, and Aparecida Barbosa Mageste. "Liquid-liquid extraction of rare earth elements using systems that are more environmentally friendly: Advances, challenges and perspectives." *Separation and Purification Technology* 282:120064(2022).<https://doi.org/10.1016/j.seppur.2021.120064>
- 10- Zhao, Qi, Zhifeng Zhang, Yanling Li, XueBian, and Wuping Liao. "Solvent extraction and separation of rare earths from chloride media using  $\alpha$ -aminophosphonic acid extractant HEHAMP." *Solvent extraction and ion exchange* 36,no.2:136-149(2018).<https://doi.org/10.1080/07366299.2018.1431079>
- 11- Opare, Emmanuel Ohene, Ethan Struhs, and Amin Mirkouei. "A comparative state-of-technology review and future directions for rare earth element separation." *Renewable and Sustainable Energy Reviews* 143: 110917(2021).<https://doi.org/10.1016/j.rser.2021.110917>
- 12- Giese, Ellen Cristine. "Biosorption as green technology for the recovery and separation of rare earth elements." *World Journal of Microbiology and Biotechnology* 36, no. 4: 1-11(2020).[doi:10.1007/s11274-020-02821-6](https://doi.org/10.1007/s11274-020-02821-6)
- 13- Rahayu, Iman, AnniAnggraeni, M. S. S. Ukun, and Husein H. Bahti. "The Effect of Pressure and Temperature on Separation of Free Gadolinium (III) From Gd-DTPA Complex by Nanofiltration-Complexation Method." In *IOP Conference Series: Materials Science and Engineering*, vol. 196, no. 1, p. 012040. IOP Publishing, 2017.DOI 10.1088/1757-899X/196/1/012040
- 14- Yin, Tai-qi, Yun Xue, Yong-de Yan, Zhen-chao Ma, Fu-qiu Ma, Mi-lin Zhang, Gui-ling Wang, and Min Qiu. "Recovery and separation of rare earth elements by molten salt electrolysis." *International Journal of Minerals, Metallurgy and Materials* 28, no.: 899-9146 (2021).[doi:10.1007/s12613-020-2228-4](https://doi.org/10.1007/s12613-020-2228-4)
- 15- Khalifa, Magdi E., Wael I. Mortada, Mohamed M. El-defrawy, and Aya A. Awad. "Selective separation of gadolinium from a series of f-block elements by cloud point extraction and its application for analysis of real samples." *Microchemical Journal* 151: 104214(2019).<https://doi.org/10.1016/j.microc.2019.104214>

- 16- Utilization of silica-chitosan nanocomposite for removal of  $^{152}\text{Eu}$  and  $^{154}\text{Eu}$  radionuclide from aqueous solutions, *J. Radioanalytical and Nuclear Chem.* 323 439–455(2020). <https://doi.org/10.1007/s10967-019-06951-6>
- 17- Evaluation of Uranium Adsorption Using Magnetic-Polyamine Chitosan from Sulfate Leach Liquor of Sela Ore Material, South Eastern Desert, Egypt, *Egyptian Journal of Chemistry* Vol. 63, No. 12. pp. 5219 - 5238 (2020). DOI: 10.21608/EJCHEM.2020.27972.2586
- 18- Highly efficient capture of Th(IV) from aqueous solutions using GO/TiO<sub>2</sub> nanocomposite *Egyptian journal of chemistry* Vol. 64, No. 3 pp. 1353 - 1362 (2021). DOI: 10.21608/EJCHEM.2020.44957.2917
- 19- Rivas, Bernabé L., Bruno F. Urbano, and Julio Sánchez. "Water-soluble and insoluble polymers, nanoparticles, nanocomposites and hybrids with ability to remove hazardous inorganic pollutants in water." *Frontiers in chemistry* 6: 320(2018). <https://doi.org/10.3389/fchem.2018.00320>
- 20- Madbouly HA, El-Hefny NE, El-Nadi YA. Adsorption and separation of terbium (III) and gadolinium (III) from aqueous nitrate medium using solid extractant. *Separation Science and Technology*. Mar 4;56(4):681-93(2021). <https://doi.org/10.1080/01496395.2018.1563614>
- 21- Zinovyev, V. G., I. A. Mitropolsky, G. I. Shulyak, P. A. Sushkov, T. M. Tyukavina, S. L. Sakharov, E. I. Malyutenkov, A. E. Tikhonova, and I. S. Okunev. "Study of the gadolinium sorption on the C100 ion-exchange resin for the development of the antineutrino detector targets." *Journal of Radioanalytical and Nuclear Chemistry* 315, no. 3: 459-473(2018). doi:10.1007/s10967-018-5703-x
- 22- rights are reserved by Ihsan, All, and Mahdi Shaheed. "Spectrophotometric Study on the Solvent Extraction of Gadolinium (III) with N-Acetylcysteine.7:3 (2016)".
- 23- CHUNHUA, X., and Y. CAIPING. "Adsorption behavior of MWAR toward Gd (III) in aqueous solution: 59-66(2010).
- 24- Sayed, Mubarak A., A. I. Helal, S. M. Abdelwahab, H. H. Mahmoud, and H. F. Aly. "Sorption and possible preconcentration of europium and gadolinium ions from aqueous solutions by Mn<sub>3</sub>O<sub>4</sub> nanoparticles." *Chemical Papers* 74, no. 2: 619-630(2020). <https://doi.org/10.1007/s11696-019-00906-7>
- 25- Fan, Q. H., D. D. Shao, J. Hu, W. S. Wu, and X. K. Wang. "Comparison of Ni<sup>2+</sup> sorption to bare and ACT-graft attapulgites: effect of pH, temperature and foreign ions." *Surface Science* 602, no. 3: 778-785(2008).<https://doi.org/10.1016/j.susc.2007.12.007>
- 26- Mohamed, Ghada M., WafaaEzzEldienRashwan, Thoria El-Nabarawy, and Abdel Naser El-Hendawy. "Removal of Basic Dyes from Aqueous Solution Onto H<sub>2</sub>SO<sub>4</sub>-modified Rice Husk." *Egyptian Journal of Chemistry* 64, no. 1: 143-155(2021). DOI: 10.21608/ejchem.2020.39613.2807
- 27- Plazinski, Wojciech, and WladyslawRudzinski. "Kinetics of adsorption at solid/solution interfaces controlled by intraparticle diffusion: a theoretical analysis." *The Journal of Physical Chemistry C* 113, no. 28: 12495-12501(2009).<https://doi.org/10.1021/jp902914z>
- 28- Nayak, Ashish Kumar, and Anjali Pal. "Development and validation of an adsorption kinetic model at solid-liquid interface using normalized Gudermannian function." *Journal of Molecular Liquids* 276: 67-77(2019).<https://doi.org/10.1016/j.molliq.2018.11.089>
- 29- Madbouly, Magdy, and A. Al-Anwar. "Tamarixaphylla Biomass as Efficient Adsorbent for

- Removal of Pb (II) Ions from Aqueous Solution: Kinetic and Applicability for Different Isotherm Models." *Egyptian Journal of Chemistry* 61, no. 1: 101-119(2018).[10.21608/EJCHEM.2018.1636.1138](https://doi.org/10.21608/EJCHEM.2018.1636.1138)
- 30- Anah, L., and N. Astrini. "Isotherm adsorption studies of Ni (II) ion removal from aqueous solutions by modified carboxymethyl cellulose hydrogel." In *IOP Conference Series: Earth and Environmental Science*, vol. 160, no. 1, p. 012017. IOP Publishing, 2018.[DOI 10.1088/1755-1315/160/1/012017](https://doi.org/10.1088/1755-1315/160/1/012017)
- 31- Khayyun, Thair Sharif, and AyadHameedMseer. "Comparison of the experimental results with the Langmuir and Freundlich models for copper removal on limestone adsorbent." *Applied Water Science* 9, no. 8: 1-8(2019). <https://doi.org/10.1007/s13201-019-1061-2>
- 32- Hu, Qili, and Zhenya Zhang. "Application of Dubinin–Radushkevich isotherm model at the solid/solution interface: A theoretical analysis." *Journal of Molecular Liquids* 277: 646-648(2019).<https://doi.org/10.1016/j.molliq.2019.01.005>
- 33- Banerjee, Sushmita, AbhijitDebnath, Bharat Kumar Allam, and Neksumi Musa. "Adsorptive and photocatalytic performance of perovskite material for the removal of food dye in an aqueous solution." *Environmental Challenges* 5: 100240(2021).<https://doi.org/10.1016/j.envc.2021.100240>
- 34- Mendes KF, editor. Interactions of Biochar and Herbicides in the Environment. *CRC Press*; 2022.
- 35- Nizam, NurulUmairah M., Marlia M. Hanafiah, EbrahimMahmoudi, Azhar A. Halim, and Abdul Wahab Mohammad. "The removal of anionic and cationic dyes from an aqueous solution using biomass-based activated carbon." *Scientific Reports* 11, no. 1: 1-17(2021).
- 36- Shikuku, Victor O., Renato Zanella, Chrispin O. Kowenje, Filipe F. Donato, Nelson MG Bandeira, and Osmar D. Prestes. "Single and binary adsorption of sulfonamide antibiotics onto iron-modified clay: linear and nonlinear isotherms, kinetics, thermodynamics, and mechanistic studies." *Applied Water Science* 8, no. 6: 1-12(2018).
- 37- Maslova, Marina V., Vladimir I. Ivanenko, Nataliya Yu Yanicheva, and Natalia V. Mudruk. "Comparison of the sorption kinetics of lead (II) and zinc (II) on titanium phosphate ion-exchanger." *International Journal of Molecular Sciences* 21, no. 2: 447(2020). <https://doi.org/10.3390/ijms21020447>
- 38- Banerjee, Sushmita, and M. C. Chattopadhyaya. "Adsorption characteristics for the removal of a toxic dye, tartrazine from aqueous solutions by a low cost agricultural by-product." *Arabian Journal of Chemistry* 10: S1629-S1638(2017).<https://doi.org/10.1016/j.arabjc.2013.06005>